ORIGINAL RESEARCH ARTICLE

Clin Pharmacokinet 2008; 47 (4): 245-259
0312-5963/08/0004-0245/$48.00/0

Identification of Intestinal Loss of a Drug through Physiologically Based Pharmacokinetic Simulation of Plasma Concentration-Time Profiles

Sheila Annie Peters

Discovery DMPK and Bioanalytical Chemistry, AstraZeneca R&D, Mölndal, Sweden

Abstract

Background and objective: Despite recent advances in understanding of the role of the gut as a metabolizing organ, recognition of gut wall metabolism and/or other factors contributing to intestinal loss of a compound has been a challenging task due to the lack of well characterized methods to distinguish it from first-pass hepatic extraction. The implications of identifying intestinal loss of a compound in drug discovery and development can be enormous. Physiologically based pharmacokinetic (PBPK) simulations of pharmacokinetic profiles provide a simple, reliable and cost-effective way to understand the mechanisms underlying pharmacokinetic processes. The purpose of this article is to demonstrate the application of PBPK simulations in bringing to light intestinal loss of orally administered drugs, using two example compounds: verapamil and an in-house compound that is no longer in development (referred to as compound A in this article).

Methods: A generic PBPK model, built in-house using MATLAB® software and incorporating absorption, metabolism, distribution, biliary and renal elimination models, was employed for simulation of concentration-time profiles. Modulation of intrinsic hepatic clearance and tissue distribution parameters in the generic PBPK model was done to achieve a good fit to the observed intravenous pharmacokinetic profiles of the compounds studied. These optimized clearance and distribution parameters are expected to be invariant across different routes of administration, as long as the kinetics are linear, and were therefore employed to simulate the oral profiles of the compounds. For compounds with reasonably good solubility and permeability, an area under the concentration-time curve for the simulated oral profile that far exceeded the observed would indicate some kind of loss in the intestine.

Results: PBPK simulations applied to compound A showed substantial loss of the compound in the gastrointestinal tract in humans but not in rats. This accounted for the lower bioavailability of the compound in humans than in rats. PBPK simulations of verapamil identified gut wall metabolism, well established in the literature, and showed large interspecies differences with respect to both gut wall metabolism and drug-induced delays in gastric emptying.

Conclusions: Mechanistic insights provided by PBPK simulations can be very valuable in answering vital questions in drug discovery and development. However, such applications of PBPK models are limited by the lack of accurate inputs for clearance and distribution. This article demonstrates a successful application of PBPK simulations to identify and quantify intestinal loss of two model compounds in rats and humans. The limitation of inaccurate inputs for the clearance and distribution parameters was overcome by optimizing these parameters through fitting intravenous profiles. The study also demonstrated that the large interspecies differences associated with gut wall metabolism and gastric emptying, evident for the compounds studied, make animal model extrapolations to humans unreliable. It is therefore important to do PBPK simulations of human pharmacokinetic profiles to understand the relevance of intestinal loss of a compound in humans.

Background

Compounds that have good permeability and solubility are generally assumed to have 100% absorption. However, intestinal loss of certain compounds through P-glycoprotein (P-gp) efflux, intestinal metabolism or a combination of both has been recognized as a factor limiting the absorption of these compounds.[1-3] The concerted action of P-gp and cytochrome P450 (CYP) 3A4 enzymes makes it difficult to assess the relative role of CYP3A4 and P-gp in determining oral drug absorption. However, for many P-gp substrates, it has been shown that P-gp has a limited role in determining intestinal absorption, contrary to previous thinking.[4-8] As P-gp is easily saturated, the contribution of P-gp to drug absorption may not be significant at clinically relevant doses – especially for high-solubility, high-permeability drugs – unless the clinical doses are very low. For these drugs at least, any intestinal loss can be attributed to metabolism by the gut flora and/or oxidative/conjugative enzymes. Several studies have demonstrated the presence of drug-metabolizing enzymes in the villus tip of enterocytes in humans and in several preclinical species.[9-13] Metabolic enzymes expressed in the enterocytes include CYPs, glucouronyltransferases, sulfotransferases and esterases. The levels of expression of drug-metabolizing enzymes in the intestine are comparable with those in the liver.[13,14] In general, enzyme-driven biotransformation is highest in the jejunum and decreases distally along the gastrointestinal (GI) tract,[15] while bacterial degradation is highest in the colon. Despite these advances in the understanding of gut wall enzymes, the importance of gut wall metabolism has been doubted,[16] due either to possible saturation effects of CYP enzymes resulting from higher lumenal drug concentrations compared with their Michaelis-Menten constant (Km) values, or to low enzyme expression and cofactor levels in the gut compared with the liver. However, there are also factors that favour intestinal metabolism over hepatic metabolism. All of the passively absorbed drug, and not just the part that perfuses the metabolizing compartment, is exposed to metabolizing enzymes in the gut. Also, the moderating effects of protein binding are absent in the gut, as all of the absorbed compound is presented to the metabolizing enzymes in the enterocytes. Gut wall metabolism is still poorly understood, as quantitative and mechanistic studies in humans are proving to be elusive. Measurement of portal vein drug concentrations, the only direct way to assess the intestinal extraction, is technically difficult. *In vitro* models are not well characterized, as there have been difficulties related to the preparation of viable enterocyte microsomes. Caco-2 cells have no measurable CYP and very little uridine diphosphate glucuronosyltransferase (UGT) activity.[12] The CYP3A4 transgenic mouse model[17] and the use of tissue slices in an Ussing chamber[18] may be good models to employ, but few such studies have been reported in the literature. The large intra- and interspecies physiological variability in the expression of drug-metabolizing enzymes in the gut[19,20] and their saturable nature introduce significant heterogeneity in the bioavailability of drugs that are metabolized by gut wall enzymes, and make interspecies extrapolation to humans less reliable. There is thus a high risk that intestinal metabolism of a compound in humans will go unrecognized because of the difficulty involved in distinguishing it from hepatic extraction. This article aims to illustrate the application of physiologically based pharmacokinetic (PBPK) simulations of pharmacokinetic profiles to identify intestinal loss of a compound using two examples: verapamil, a compound in which intestinal metabolism has been well established,[21] and an in-house compound from AstraZeneca that is no longer in development (compound A). In addition to this primary aim, the article also discusses the application of PBPK in identifying enterohepatic recirculation and gastric emptying delay, the two pharmacokinetic processes that also affect the concentration-time profiles (lineshapes) of the oral plasma curves of these compounds.

Verapamil is a CYP3A4-metabolized, high-clearance drug. Its low and variable bioavailability has been attributed to an interplay of intestinal CYP3A4 metabolism and P-gp efflux.[22] However, as for many other drugs, the role of P-gp in determining the extent of absorption of this compound has been debated.[6,8] On the other hand, there is good experimental evidence of a substantial contribution of intestinal first-pass metabolism in determining the oral bioavailability of verapamil.[23] PBPK simulations have been applied to the pharmacokinetic profiles of *R*- and *S*-verapamil in rats and to *R*-, *S*- and racaemic verapamil in humans to see if such simulations can help identify the intestinal loss of verapamil reported in the literature.

Compound A has good efficacy but poor bioavailability in humans. PBPK simulations of its rat and human pharmacokinetic profiles were done to identify possible reasons for its poor bioavailability. The lineshape of the oral plasma curve of compound A in humans is influenced by both intestinal loss and enterohepatic recirculation.

The PBPK[24-26] approach can be used for predictions or for simulation of pharmacokinetic (concentration-time) profiles. As a prediction tool, its value is limited by the lack of reliable input parameters, especially for clearance, where the *in vitro* measurements for intrinsic clearance rarely match up to the *in vivo*. The difficulty in getting experimental measures of tissue partition coefficients is a further deterrent to using PBPK modelling for predictions. In a simulation, however, the focus is not on quantitative predictions; instead, the emphasis is on gaining valuable insights into processes that drive the pharmacokinetics of a compound. The oral pharmacokinetic profile of a compound can be simulated using the optimized clearance and distribution parameters that are obtained through fitting the observed intravenous pharmacokinetic profile, in combination with the physicochemical properties, measured or calculated permeability, and measured

solubility of the compound. As long as solubility and permeability are the only parameters that determine the oral lineshape, the simulated oral lineshapes show reasonable agreement with the observed.[27] Consequently, any mismatch between simulated and observed oral lineshapes should reflect complications arising from factors such as drug-induced gastric emptying delay, gut wall metabolism, P-gp efflux, chemical degradation, enterohepatic recirculation and variable absorption across the gut.[27] The utility of this approach in identifying the well established intestinal loss in verapamil has been tested, as a kind of validation of the approach, before being applied to compound A. Through these examples, this article aims to establish the value of PBPK simulations for quantitative identification of intestinal loss of compounds and to show that simulations of human oral pharmacokinetic profiles are vital to assessment of the role of the gut in reducing the bioavailability of compounds in humans. The study also aims to demonstrate that lack of reliable tissue partition coefficients and clearance parameters need not be a deterrent to the application of whole-body PBPK modelling in drug discovery and development projects, to unravel mechanistic information from pharmacokinetic data.

Methods

Physiologically Based Pharmacokinetic (PBPK) Model Structure

A generic PBPK model (figure 1), built in-house using MATLAB® software (The MathWorks, Inc., Natick, MA, USA),[27] was used in all simulations reported in this article. Incorporated into this model were models for absorption, distribution, metabolism and excretion. To facilitate hypothesis testing

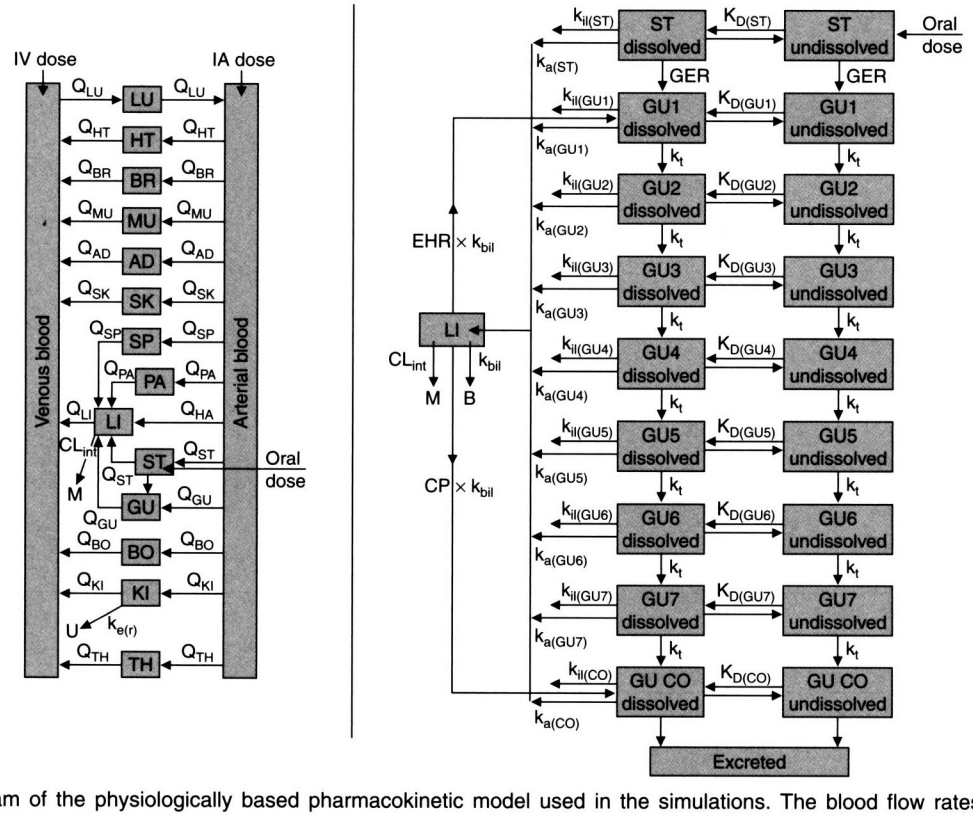

Fig. 1. Schematic diagram of the physiologically based pharmacokinetic model used in the simulations. The blood flow rates associated with the 14 compartments – lung (LU), heart (HT), brain (BR), muscle (MU), adipose tissue (AD), skin (SK), spleen (SP), pancreas (PA), liver (LI), stomach (ST), gut (GU), bone (BO), kidney (KI) and thymus (TH) – are represented by Q, subscripted with the appropriate compartment. The intravenous (IV) dose enters the venous compartment and the intra-arterial (IA) dose enters the arterial compartment, while the oral dose enters the stomach compartment. The intrinsic clearance (CL_{int}) rate governs the rate of conversion to the metabolite (M). $k_{e(r)}$ is the renal elimination rate constant that determines the amount eliminated in the urine (U). The somatic model on the left is linked to an absorption model (shown on the right) through the liver compartment. GU1–GU7 represent the seven small intestinal compartments. The colonic (GU CO) and stomach (ST) compartments are also included to consider colonic and gastric absorptions. k_a and k_{il} represent the rates of absorption and intestinal loss for the different gastrointestinal compartments, respectively. A non-zero fraction to consider metabolite conversion to the parent (CP) in the colon may also be used if necessary. EHR is the enterohepatic recirculation constant that switches between 1 and 0 to include or exclude emptying of the parent compound into the duodenal compartment (GU1). **B** = amount of the compound eliminated as the metabolite in the bile; **GER** = gastric emptying rate constant; **HA** = hepatic artery; $\mathbf{k_{bil}}$ = rate of emptying of the parent compound or its metabolite into the bile; $\mathbf{K_D}$ = dissolution rate constant; $\mathbf{k_t}$ = transit rate constant.

Table I. Summary of data for verapamil and compound A used in physiologically based pharmacokinetic simulations[a]

Parameter	Verapamil			Compound A
	R-	*S*-	racaemic	
Compound-dependent properties				
Molecular weight (Da)			455	446.5
log P			3.96	3
K_p factor used in rat simulations	1	1		1
K_p factor used in human simulations	0.55	0.39	0.39	0.7
Base pKa			8.7	9.7
Solubility at pH 7.4 (mmol/L)			3	0.449
Caco-2 permeability ($\times 10^{-6}$ cm/sec)			10	1.9
Caco-2 permeability with quinidine ($\times 10^{-6}$ cm/sec)				5.8
Rat				
Permeability actually used in simulations ($\times 10^{-6}$ cm/sec)			10	5
Fraction of free drug in plasma	0.064	0.062	ND	0.65
In vitro microsomal CL_{int} (mL/min/kg)				85
CL_{int} used in simulations (mL/min/kg)	1260	800	ND	441
Blood : plasma ratio			0.75	1.23
Intravenous dose (mg)			0.11	0.68
Oral dose (mg)			1.1	3.35
Bioavailability (%)	4.1 ± 1.1	7.4 ± 3.1	ND	36 ± 7
Human				
Permeability actually used in simulations ($\times 10^{-6}$ cm/sec)			10	5.8
Fraction of free drug in plasma	0.064	0.11	0.1	0.34
In vitro microsomal CL_{int} (mL/min/kg)				8.2
CL_{int} used in simulations (mL/min/kg)	331	302	165	60
Blood : plasma ratio			0.75	1
Intravenous dose (mg)	50	10	10	100
Oral dose (mg)	480	120	120	500
Total plasma clearance (mL/min/kg)	13.5 ± 1.5	18.2 ± 1.8	10.4 ± 3.3	16 ± 1.7
Renal clearance (mL/min/kg)				2.9 ± 0.3
Fraction of compound excreted unchanged in urine				0.17 ± 0.01
Bioavailability (%)	67	16	19.8 ± 15.1	16 ± 4

a Values are expressed as mean ± SD.

CL_{int} = intrinsic clearance; **K_p factor** = a multiplicative factor used to reduce or increase the tissue distribution coefficients; **log P** = octanol-water partition coefficient; **ND** = no data; **pKa** = acid dissociation constant.

through simulation of pharmacokinetic lineshapes, the absorption model had additional features such as intestinal loss, renal and biliary elimination, enterohepatic recirculation and metabolite conversion to the parent in the distal GI tract. First-order intestinal loss rate constants were introduced into all nine compartments to take into account possible loss of a compound from the intestine due to P-gp efflux, intestinal metabolism or chemical degradation. To start with, the intestinal loss rate constants were considered to be zero.

PBPK Model Parameters

The physiological parameters employed in the model were taken from the literature.[27]

In Vivo Pharmacokinetic Data

All data employed in the PBPK simulation of the pharmacokinetic profiles of verapamil and compound A are summarized in table I. In the case of verapamil, literature values were used as the input for parameters such as the fraction of the free drug in plasma in humans[28] and rats,[29] Caco-2 permeability,[30] octanol-water

partition coefficient (log P),[31] acid dissociation constant (pKa)[31] and solubility.[6] For compound A, these properties were measured in-house. The Caco-2 permeability measured for compound A with quinidine used a high enough concentration of quinidine to saturate the P-gp completely. The *in vivo* pharmacokinetic data for the *R*- and *S*-verapamil enantiomers in rats[32] and in humans[28,33,34] were obtained from the literature. The choice of these references for the pharmacokinetics of verapamil was dictated by the need to find the most recent data reported separately for the two enantiomers, to enable comparison of the results for the enantiomers. Older reports dealt only with racaemic verapamil. The observed rat pharmacokinetic data reported here are the averages of the data collected from six animals for each of the enantiomers. Human pharmacokinetic data for the enantiomers were studied in five healthy volunteers following intravenous administration[28] and in eight healthy volunteers following oral administration,[33] while the pharmacokinetic data for racaemic verapamil were from 20 young men with a mean age of 25.2 ± 3.6 years.[34] The rat and human pharmacokinetic data for compound A were generated in-house. The rat intravenous and oral pharmacokinetic data were obtained from three rats. The clinical pharmacokinetic studies were done on five healthy volunteers following oral administration and four healthy volunteers following an intravenous infusion lasting 1 hour. The oral pharmacokinetic data in all cases corresponded to the fasted state. The *in vivo* pharmacokinetic doses used in all of these studies are presented in table I.

PBPK Simulations

Parameterization through Fitting an Intravenous Profile

An intravenous profile is determined only by the distribution, metabolism and excretion kinetics of the compound. So, to start with, an intravenous plasma profile of a compound of interest is simulated using the input parameters shown in table I. If the area under the concentration-time curve (AUC) of the simulated curve differs from that of the observed, it indicates that the *in vitro* intrinsic clearance (CL_{int}) cannot explain the observed clearance. Therefore, the CL_{int} is modulated till the AUCs match. Since the distribution and clearance parameters affect different aspects of the overall shape of the concentration-time profile, parameters affecting these can be modulated independently of each other. If the fraction of the intravenously administered compound excreted unchanged renally (f_e) is not known, it is reasonable to assume that the compound has only hepatic clearance as long as the compound is sufficiently lipophilic. If the f_e is non-zero, the renal elimination rate constant is modulated to reproduce the observed f_e.[27] If the lineshapes do not match despite the AUCs being the same, it indicates that the distribution coefficients used in the simulation cannot account for the observed distribution. This could be due to the role of transporters in tissue distribution. Alternatively, distribution into the tissues could be less than what one would expect from the lipophilicity of the compound if there were a permeability limitation (diffusion barriers) to the distribution of the compound into the tissues.[35] Distribution into the tissues could also be greater than what is expected from lipophilicity if specific binding to one or more tissues is important for a compound. A multiplicative factor for the tissue partitioning coefficient (K_p factor) is used to reduce or increase the tissue distribution coefficients of all 14 organs represented as compartments in the PBPK model, in order to get a good fit to the observed profile. Goodness of fit is judged by ensuring good agreement of the calculated AUC with the mean of the observed, as well as through calculation of the reduced χ^2 statistic (equation 1), if a measure of physiological variabilities is available (either multiple observations or their standard deviations), or otherwise by minimizing the mean fold error (equation 2):

$$\chi^2 = \frac{1}{N}\sum_{i=1}^{N}\left(\frac{\Delta_i^2}{\sigma_i^2}\right) \quad \text{(Eq. 1)}$$

$$\text{Mean fold error} = 10^{\left[\frac{1}{n}\Sigma \log (\text{fold error})\right]} \quad \text{(Eq. 2)}$$

where i is any one of the N number of observations, Δ is the difference between the observed and predicted values at the same timepoints, and σ is the standard deviation at the corresponding timepoints. As the square of the deviations from the observed at each timepoint is expected to agree with the observed variance (σ^2) at that timepoint, χ^2 should be close to 1 for a good fit. The second measure of accuracy is the mean fold error (equation 2). A fold error is estimated for every timepoint by taking the ratio of the predicted and observed values, such that it is always greater than 1.

Once the intravenous fit is in place, the oral profile is simulated using the optimized clearance and distribution parameters from the best intravenous fit. The assumption here is that the intrinsic clearance rates and tissue distribution coefficients can be expected to be invariant across different routes of administration for therapeutic concentrations. Simulation of an oral profile should handle the additional complexity arising from the absorption phase, which is influenced by an array of physiological factors such as the gastric emptying time, intestinal transit kinetics, P-gp efflux, gut wall enzymes and transporters, apart from compound characteristics.

Simulation of the Oral Profile: Getting Intestinal Loss Rate Constants and Gastric Emptying Rate Constants

The parameters affecting clearance and distribution are now fixed, and these are used to simulate an oral profile. Comparison of the simulated oral profile with the observed should give some idea as to which of the multitude of parameters affecting the oral profile

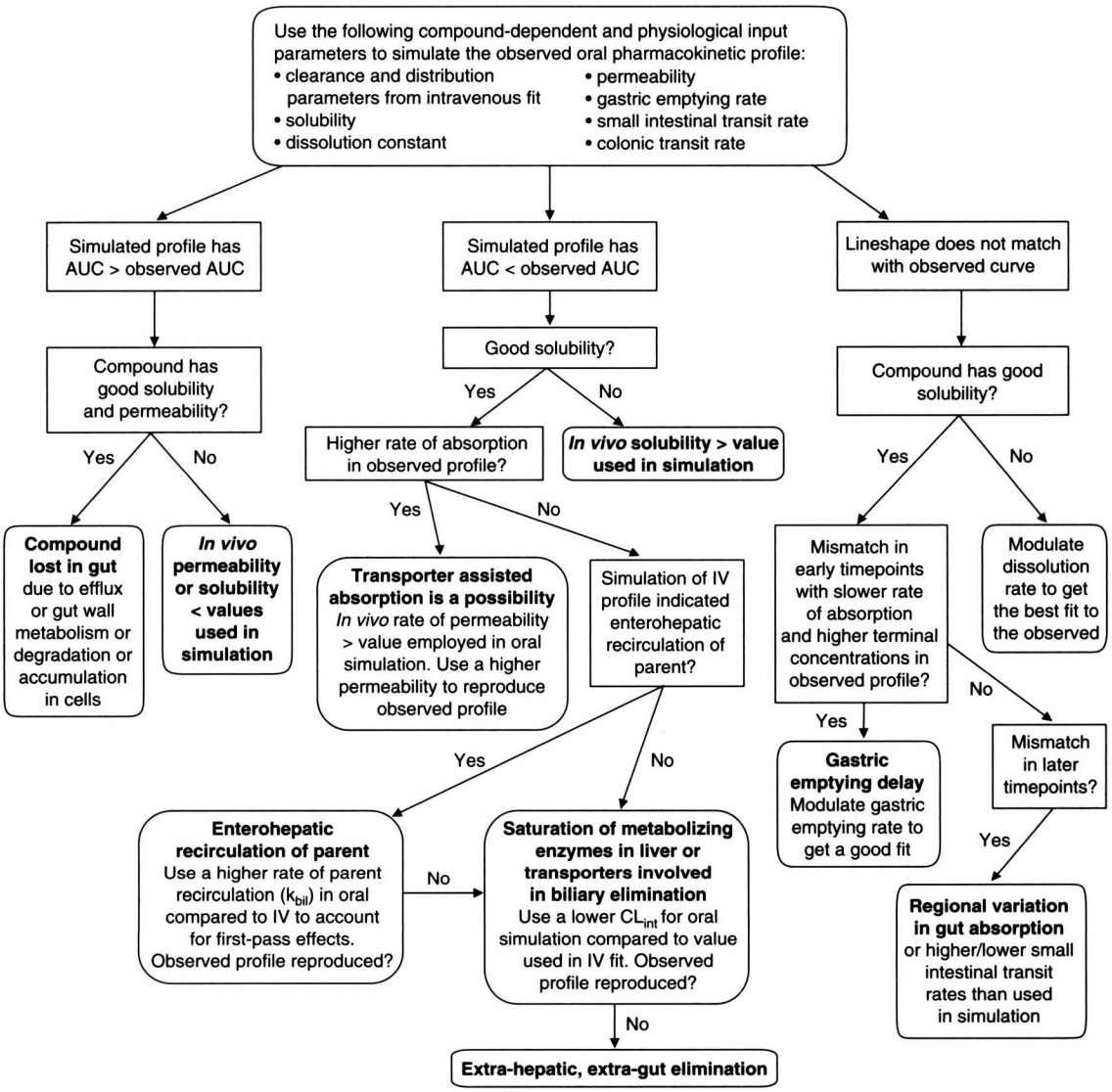

Fig. 2. Decision tree analysis leading to identification of different mechanisms that affect oral lineshapes. The branches of the decision tree that lead to intestinal loss and gastric emptying delay are the paths of interest in this study. **AUC** = area under the concentration-time curve; **CL_{int}** = intrinsic clearance; **IV** = intravenous; **k_{bil}** = rate of emptying of the parent compound or its metabolite into the bile.

can be modulated in order to reproduce the observed profile. Figure 2 illustrates how the different mechanisms affecting oral lineshapes can be identified. A simulated AUC that is substantially greater than the observed is indicative of intestinal loss due to either degradation, gut wall metabolism and/or P-gp efflux. Intestinal loss rate constants are then included in the model and arbitrarily adjusted to get the best fit to the observed oral profile. The gastric emptying rate, intestinal transit kinetics and variable permeability and/or dissolution kinetics along the GI tract have a profound effect on the shape of the oral profile. However, intestinal transit kinetics are fairly constant, and that leaves parameters affecting the gastric emptying rate or permeability and/or solubility as the only other parameters that need to be adjusted to reproduce the oral profile. These have completely different effects on the lineshape and can thus be varied independently of each other. A gastric emptying rate that is lower than the average normal value has the effect of slowing the rate of the initial upswing of the absorption phase, but the terminal phase is characterized by higher than expected concentrations.[36] Thus, impaired gastric emptying has the effect of flattening the oral profile and can be easily distinguished from lineshape changes accompanying a variable absorption rate arising from the variability of solubility and/or permeability along the GI tract. If comparison of the predicted with the observed oral profile suggests delayed gastric emptying, the gastric emptying rates are reduced till the predicted profile shows a reasonable level of agreement with the observed.

Calculation of the Intestinal Loss Fraction

Compounds that have good solubility and good permeability are consequently expected to have complete absorption. Any reduction in the fraction absorbed can be directly related to the intestinal loss fraction. The absorption model incorporated in the PBPK model provides an estimate of the fraction of the dose absorbed by summing the fraction of the dose absorbed in each of the nine GI compartments. The intestinal loss fraction is obtained according to equation 3, using the fraction (f) of the dose absorbed values from two simulations, one with inclusion of intestinal loss rate constants (k_{il}) and the other without inclusion of intestinal loss rate constants:

$$\text{Intestinal loss fraction} = f_{\text{without } k_{il}} - f_{\text{with } k_{il}} \quad \text{(Eq. 3)}$$

Calculation of the Hepatic Extraction Ratio

Hepatic clearance (CL_H) is obtained by subtracting renal clearance from total clearance. Using hepatic blood flow rates (Q_H) in rats and humans,[27] the hepatic extraction ratio is calculated according to equation 4:

$$\text{Hepatic extraction ratio} = \frac{CL_H}{Q_H} \quad \text{(Eq. 4)}$$

Parameter Sensitivity Analysis

A formal parameter sensitivity analysis has been presented to demonstrate that agreement with the observed curve could be achieved only by modulation of parameters that cause an increased AUC. All of the input parameters that affect the oral lineshape, such as the dissolution constant, solubility of the compound, absorption rate constant, gastric emptying rate, intestinal transit rate and colonic transit rate, were varied individually over a wide range of values by multiplying them by factors (0.01, 0.02, 0.05, 0.1, 0.2, 0.5, 1, 2, 5, 10, 20, 50, 100). The effect of these variations on the AUC was studied.

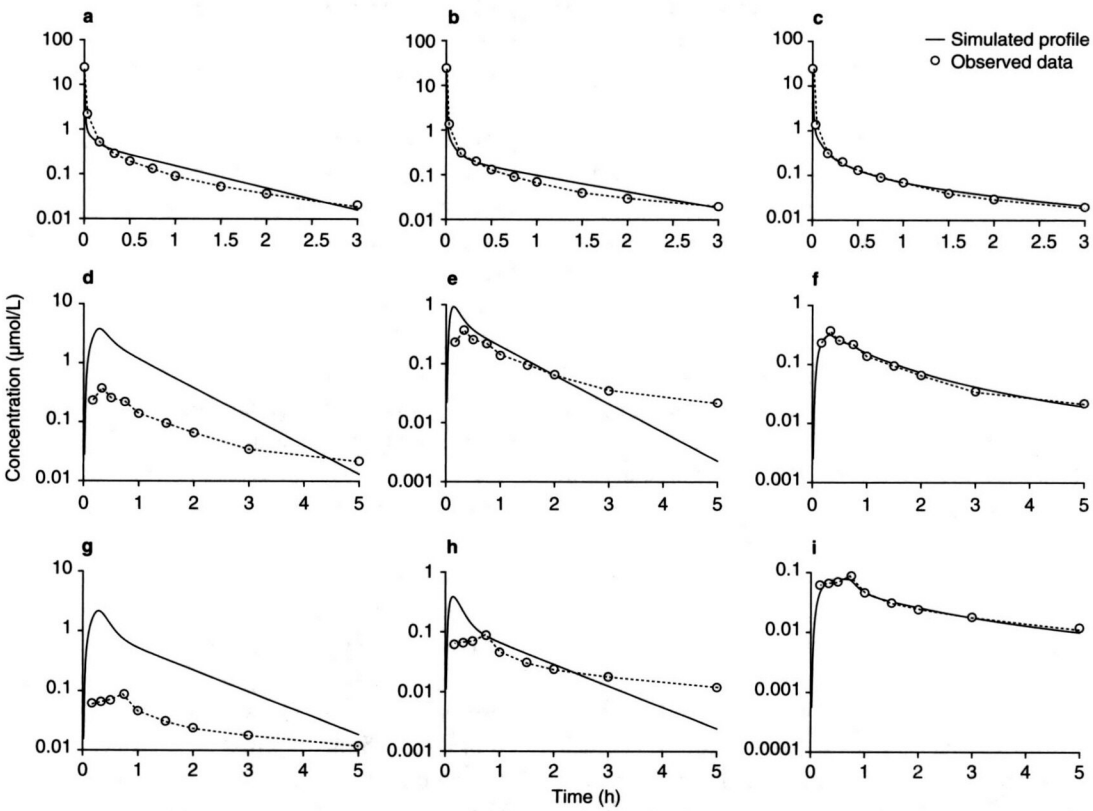

Fig. 3. Physiologically based pharmacokinetic (PBPK) simulations of pharmacokinetic profiles of verapamil in rats. (**a**) Simulation of the intravenous profile of *S*-verapamil. (**b**) Simulation of the intravenous profile of *R*-verapamil. (**c**) Refined PBPK simulations of the intravenous profile of *R*-verapamil. (**d**) Simulated oral profile of *S*-verapamil against the observed when neither intestinal loss nor gastric emptying delay was considered. (**e**) Oral simulation excluding gastric emptying delay and including intestinal loss for *S*-verapamil. (**f**) Oral simulation with both intestinal loss and gastric emptying delay included for *S*-verapamil. Panels (**g**), (**h**) and (**i**) correspond to (**d**), (**e**) and (**f**) for *R*-verapamil.

Table II. Gastric emptying rate constants and intestinal loss rate constants used in physiologically based pharmacokinetic simulations

Species	Gastric emptying rate constants[a] (min^{-1})			Intestinal loss rate constants[a] (min^{-1})			
	Verapamil			Verapamil			Compound A
	R-	*S*-	racaemic	*R*-	*S*-	racaemic	
Rat	0.018, 0.003[b]	0.04, 0.015, 0.0045[c]	ND	2.5	1.67	ND	ND
Human	0.009	0.009	0.009	0	0.14	0.19	0.1

a The rate constants are not numerically comparable across species.

b Time-dependent gastric emptying rates after 0 and 0.7 h of oral administration, respectively.

c Time-dependent gastric emptying rates after 0, 0.3 and 0.7 h of oral administration, respectively.

ND = no data.

Results

Simulation of the Plasma Concentration-Time Curves of *R*- and *S*-Verapamil in Rats

The PBPK simulations of the pharmacokinetic profiles of verapamil in rats are shown in figure 3. As described in the Methods section, a good fit to the intravenous profile observed in rats was first obtained with modulations in CL_{int} and the K_p factor (figures 3a and 3b). A K_p factor of 1 was used, suggesting that the distribution of the compound was consistent with its lipophilicity and the fraction unbound in plasma. Better fits could be obtained (figure 3c) by considering a greater partitioning of the drug into slow-perfused organs, such as adipose tissue or muscle, to explain the slower initial distribution of the drug and its longer retention in these tissues as seen in the observed curve. However, such a refinement made only a marginal difference to the results.

Input parameters from the best intravenous fit were thus fixed for simulating the oral profiles. Simulation of the oral dose profiles of *S*- and *R*-verapamil showed that there was a mismatch in the lineshapes between the simulated and the observed pharmacokinetic profiles (figures 3d and 3g). The AUC of the simulated oral profile was much higher than that of the observed. This implied that there was a much greater loss of the compound from the intestine than what would be expected just from first-pass hepatic extraction, which the physiological model takes into account. Therefore, appropriate intestinal loss rate constants were used for all of the intestinal compartments of the PBPK model (see table II) in order to get the best fit to the observed.

In figures 3e and 3h, where the oral profiles have been simulated with intestinal loss constants, the observed profile seems to be characterized by a lower rate of absorption, compared with the simulated profile. This is manifest in the longer times to reach maximum concentrations of 20 ± 6.3 minutes and approximately 30 ± 12 minutes for the *S*- and the *R*-verapamil enantiomers[32] for the observed curve, compared with approximately 10 minutes for the simulated and prolonged absorption phases of the observed curve, resulting in its higher terminal concentrations compared with the simulation. This discrepancy is typical of a compound that inhibits the gastric emptying rate.[36] By reducing the gastric emptying rate from the initial value of 0.37 min^{-1} that is characteristic for rats,[27] better fits could be obtained (figures 3f and 3i).

Simulation of the Plasma Concentration-Time Curves of *R*-, *S*- and Racaemic Verapamil in Humans

The PBPK simulations of the pharmacokinetic profiles of *S*-verapamil in humans are shown in figure 4. A lower K_p factor (table I) was used to get a good fit to the observed intravenous profile, suggesting that the distribution of verapamil in humans is restricted compared with what would be expected from its lipophilicity. The CL_{int} and K_p factor from the best fit to the observed intravenous profile were fixed for simulation of the oral profile (figure 4b). The simulation results (table II), though somewhat similar to those observed in rats, also showed marked differences with respect to the extent of intestinal loss of *R*- and *S*-verapamil. No refinement was attempted to correct the mismatch between the observed and simulated profiles (figure 4c), which was probably due to a short lag time after which gastric emptying commenced. Figures 4d and 4e show simulations considering intestinal loss and gastric emptying delays separately. Simulations of *R*-verapamil in humans showed no intestinal loss but only gastric emptying impairment (figure 5).

The simulations of racaemic verapamil in humans (figure 6) were done on pharmacokinetic profiles obtained from a different literature source from that of *R*- and *S*-verapamil. The racaemic verapamil data were accompanied by standard deviations.

Parameter sensitivity analysis was done to see the effect of all parameters affecting an oral profile on the AUC of racaemic verapamil in humans. Figure 7 shows that solubility and the absorption rate constant were the only two parameters that affected the AUC. Solubility had to be reduced to less than one tenth of the value used in the simulation in order to see any effect on the AUC. Reducing the absorption rate constant tended to reduce the AUC from the simulated value of nearly 4 μmol • h/L to the observed value of 0.92 μmol • h/L. However, there is no rationale to assume that the solubility and permeability (and therefore the absorption rate constant) of verapamil would be altered to such

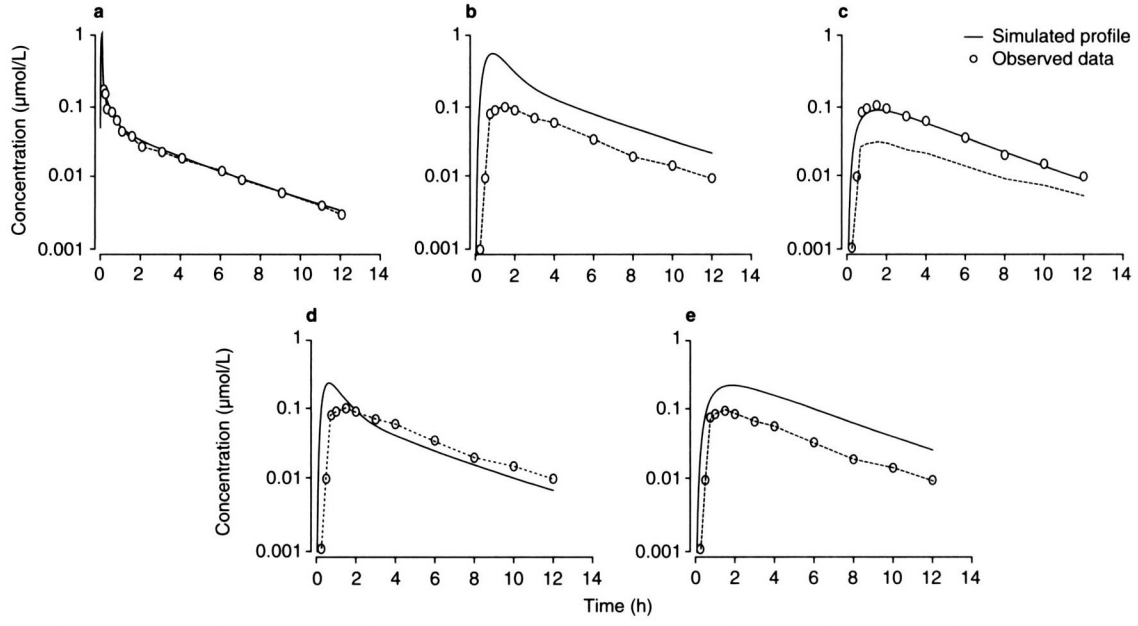

Fig. 4. Physiologically based pharmacokinetic simulations of pharmacokinetic profiles of *S*-verapamil in humans. (**a**) Simulation of the intravenous profile. (**b**) Simulated oral profile against the observed when neither intestinal loss nor gastric emptying delay was considered. (**c**) Simulation of the oral profile with intestinal loss rate constants introduced and using a reduced gastric emptying rate. (**d**) Simulation of the oral profile with an intestinal loss rate constant but excluding gastric emptying delay. (**e**) Simulation of the oral profile with a reduced gastric emptying rate but excluding intestinal loss.

low values *in vivo*. The introduction of intestinal loss constants in each of the GI compartments is therefore necessary to simulate the observed lineshape.

Simulation of the Plasma Concentration-Time Curves of Compound A in Rats

A good fit to the observed intravenous profile of compound A in rats (figure 8a) needed a much higher CL_{int} than what was measured *in vitro* (table I). As the deviation of the PBPK simulated oral plasma concentration-time curve from the mean profile for this compound in rats (figure 8b) was within the physiological variability, any further refinements would not be significant.

Simulation of the Plasma Concentration-Time Curves of Compound A in Humans

Simulation of the intravenous profile of compound A (figure 9a) was done using a much higher CL_{int} than what was measured *in vitro* (table I) and a slightly lower K_p factor. Since 17% of the compound was known to be excreted in the urine unchanged, it was important to use an appropriate renal elimination constant, as otherwise a higher proportion of the drug would be extracted in the liver compartment than what prevails *in vivo*. The terminal part of the intravenous curve tended to have higher than expected concentrations in the observed profile. This could come about if the compound is recirculated enterohepatically. Figure 9b shows the simulation with the inclusion of the rate constant for enterohepatic recirculation. Figures 9c and 9d demonstrate the effect of using Caco-2 permeability with and without quinidine on the simulation

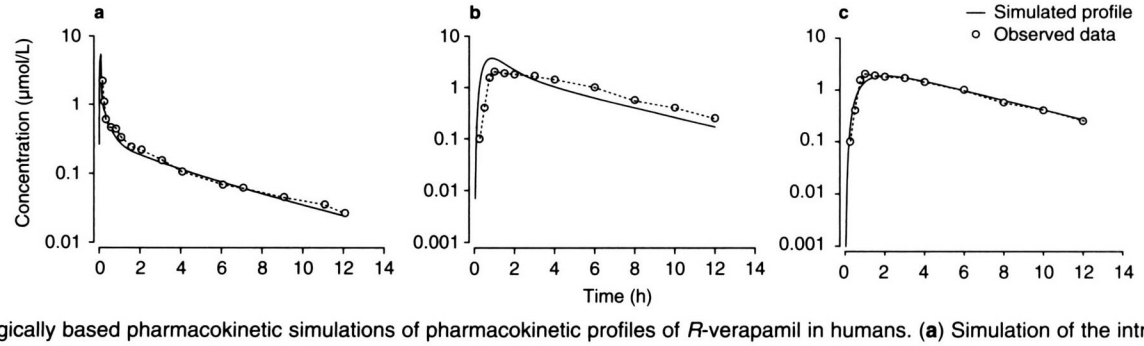

Fig. 5. Physiologically based pharmacokinetic simulations of pharmacokinetic profiles of *R*-verapamil in humans. (**a**) Simulation of the intravenous profile. (**b**) Simulated oral profile against the observed when gastric emptying delay was not considered. (**c**) Oral simulation with gastric emptying delay included.

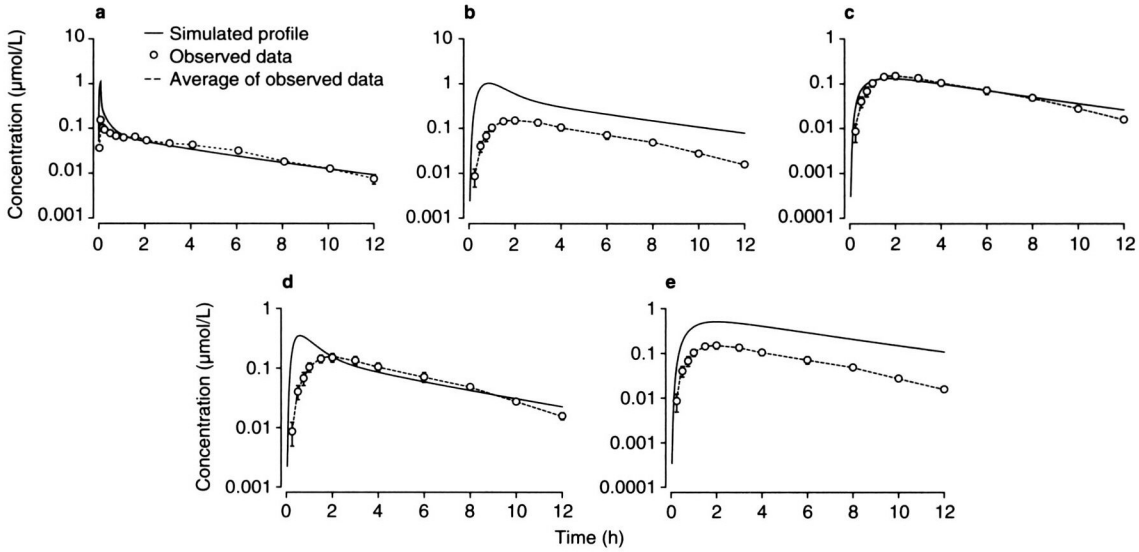

Fig. 6. Physiologically based pharmacokinetic simulations of pharmacokinetic profiles of racaemic verapamil in humans. (**a**) Simulation of the intravenous profile. (**b**) Simulated oral profile against the observed when neither intestinal loss nor gastric emptying delay was considered. (**c**) Simulation of the oral profile with intestinal loss rate constants introduced and with a reduced gastric emptying rate. (**d**) Simulation of the oral profile with an intestinal loss rate constant but excluding gastric emptying delay. (**e**) Simulation of the oral profile with a reduced gastric emptying rate but excluding intestinal loss.

of the oral profile of compound A. The former seemed to fit better. This points to the limited role of P-gp in determining absorption, at least in the proximal small intestine. The area under the simulated curve was much greater than that under the observed plasma curve. Clearly, this is indicative of intestinal metabolism if P-gp does not have a significant role. Therefore, intestinal loss rate constants were introduced for the intestinal compartments in the model (table II). In addition, enterohepatic recirculation of the compound was also incorporated in order to reproduce the observed profile (figure 9e). The enterohepatic recirculation model within the PBPK model was quite crude and did not take into account saturation effects. This explains the poor agreement between the simulated and observed terminal parts of the curves. Figures 9f and 9g show the simulated profiles including intestinal loss but without considering enterohepatic recirculation, and including enterohepatic recirculation but excluding intestinal loss. Parameter sensitivity analysis for compound A gave results similar to those for verapamil; therefore, those results are not reported.

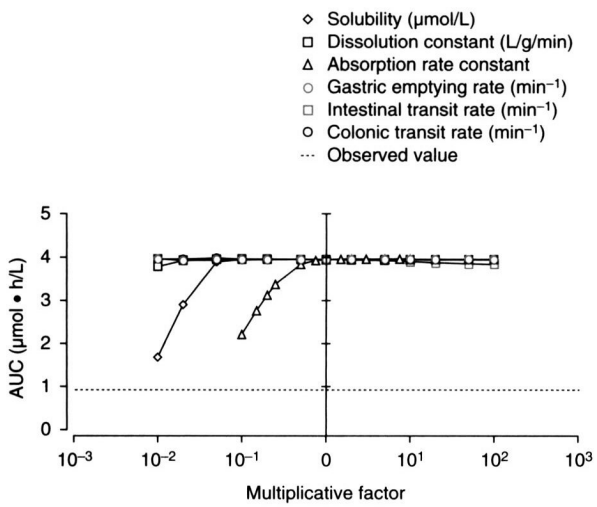

Fig. 7. Parameter sensitivity analysis of racaemic verapamil in humans. The multiplicative factor is the factor by which an input parameter was multiplied. The solubility and absorption rate constant were the only parameters that had the potential to reduce the area under the curve (AUC) from the simulated value of nearly 4 μmol • h/L to the observed value of 0.92 μmol • h/L.

Intestinal Loss Fraction

The intestinal loss fractions calculated for verapamil and compound A are presented in table III. The fraction absorbed from PBPK simulations without inclusion of intestinal loss constants for verapamil, irrespective of the species or enantiomer, was 1. Using the fraction absorbed obtained from PBPK simulations with inclusion of intestinal loss constants, the intestinal loss fractions were computed as outlined in the methods section. The intestinal loss fraction for verapamil in rats is not available in the literature. For humans, it is reported to be 0.49,[21] which agrees very well with the results obtained from PBPK simulations.

For compound A, the fraction absorbed from PBPK simulations with inclusion of intestinal loss constants (corresponding to figure 9e) was 0.45. The fraction absorbed for the compound from PBPK simulations without inclusion of intestinal loss constants was 1. The intestinal loss fraction for the compound from PBPK simulations was therefore 0.55. The hepatic extraction ratio in humans, calculated on the assumption that all non-renal elimination came

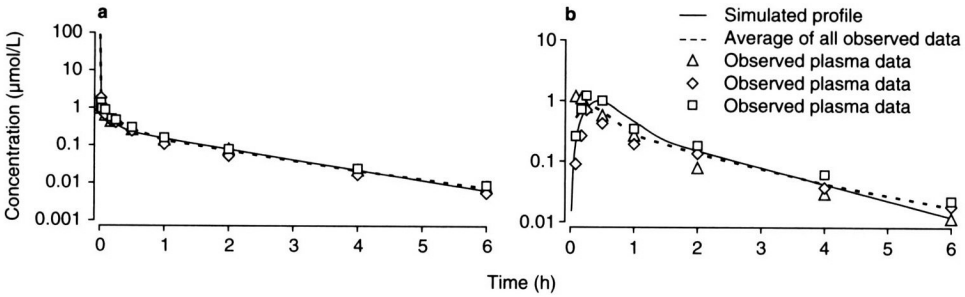

Fig. 8. Physiologically based pharmacokinetic simulations of pharmacokinetic profiles of compound A in rats. Simulations of (**a**) intravenous and (**b**) oral profiles against the observed data from different animals.

from the liver, was 0.55. Based on this, the compound should have had a bioavailability of 45%. However, the observed bioavailability was only 16%. This observed value could be explained only by the inclusion of the intestinal loss fraction.

Summary Results

Verapamil

Calcium channel antagonists have been known to delay gastric emptying rates in both rats[37] and humans[38-40] through inhibition of gastric smooth muscle contraction.[38] PBPK simulations of verapamil were able to reveal gastric emptying delays reflected in its oral pharmacokinetic profiles in both species. While a time-

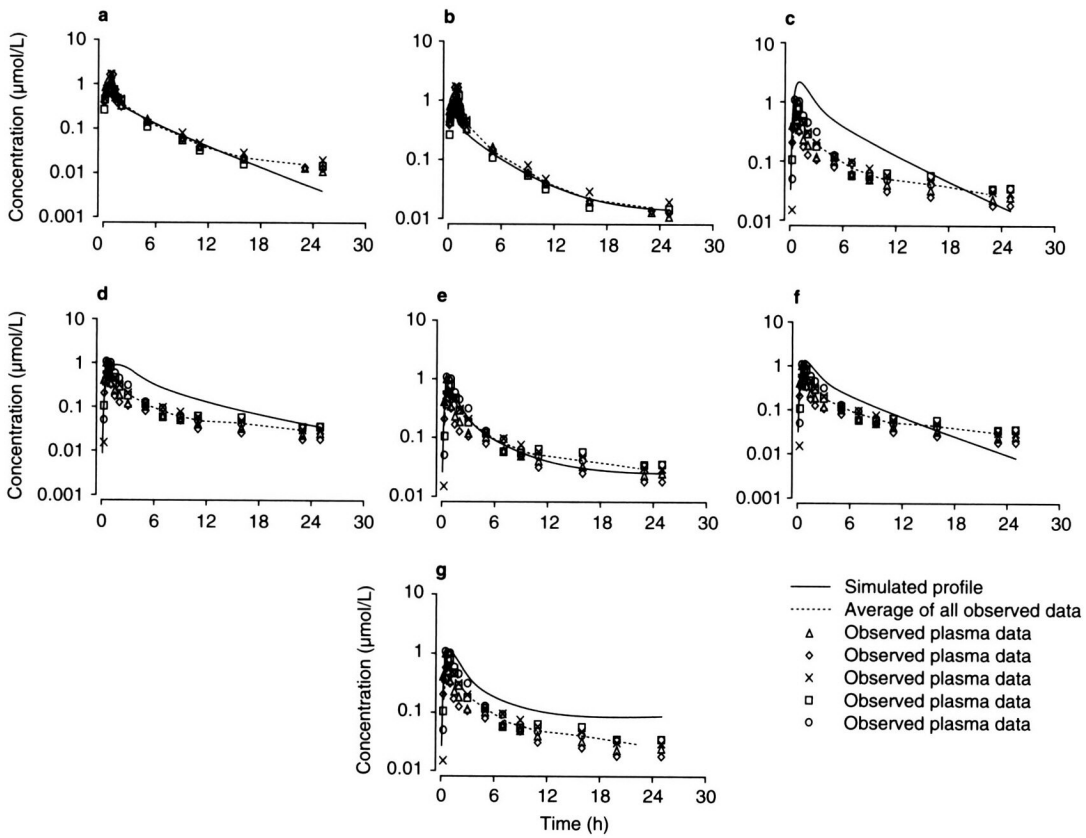

Fig. 9. Physiologically based pharmacokinetic simulations of pharmacokinetic profiles of compound A in humans. (**a**) Simulation of the intravenous profile without enterohepatic recirculation. (**b**) Simulation of the intravenous profile with inclusion of enterohepatic recirculation. (**c**) Simulated oral profile against the observed when intestinal loss was not considered; the permeability used was 5.8 cm/sec. (**d**) Simulated oral profile against the observed when intestinal loss was not considered; the permeability used was 1.9 cm/sec. (**e**) Simulation of the oral profile with intestinal loss rate constants introduced and refinement with enterohepatic recirculation. (**f**) Simulation of the oral profile excluding enterohepatic recirculation and including intestinal loss. (**g**) Simulation of the oral profile including enterohepatic recirculation and excluding intestinal loss.

Table III. Intestinal loss fractions from physiologically based pharmacokinetic simulations

Species	Verapamil			Compound A
	R-	*S*-	racaemic	
Rat	0.79	0.75	ND	ND
Human	0	0.5	0.5	0.55

ND = no data.

dependent emptying rate constant was used for simulating the rat profiles, a single rate constant was sufficient for the human profiles. In rats, gastric emptying delays seemed to be slightly greater for the *S*-enantiomer than for the *R*-enantiomer, while in humans there was no difference between *R*-, *S*- and racaemic verapamil.

PBPK simulations of the *R*- and *S*-enantiomers of verapamil in rats and humans showed that intestinal loss in rats was more or less comparable for the *R*- and *S*-enantiomers, while in humans it was nonexistent for the *R*-enantiomer and rather high for the *S*-enantiomer (table III). This highlights the high species variability of intestinal loss. The observed intestinal loss could be due to P-gp efflux or due to intestinal metabolism mediated by intestinal drug-metabolizing enzymes. As the role of P-gp has been shown to be minimal in verapamil,[6] it is quite likely that the intestinal loss of verapamil is predominantly due to intestinal metabolism. In humans, racaemic verapamil should have had an intestinal loss fraction of 0.25 (the average of the values for the *R*- and *S*-enantiomers). The observed discrepancy could perhaps be attributed to the different sources of oral *in vivo* pharmacokinetic data employed for the PBPK simulations of *R*-, *S*- and racaemic verapamil.

Compound A

PBPK simulations of human pharmacokinetic profiles of compound A showed substantial intestinal loss of the compound in humans, while only hepatic metabolism dominated in rats. This was also reflected in the higher bioavailability of the compound in rats than in humans. Like verapamil, compound A also has very different intestinal loss profiles in rats and humans.

Although the origin of intestinal loss of the compound could not be established through experiments, it is highly probable that it could be attributed to gut wall metabolism. The predominant metabolite for compound A was its ether glucuronide. Only negligible amounts of other metabolites were formed. The presence of glucuronidating enzymes in the intestinal wall has been established in several species.[12,16,41-43] Although uridine diphosphate glucuronic acid (the cofactor necessary for the UGT enzymes) is reported to be 15–50 times lesser in the gut and UGT levels are overall 30 times greater in the liver – except for UGT1A levels, which are comparable to those in the liver – many examples of intestinal glucuronidation have been reported.[44-46] Attempts to obtain experimental proof of intestinal metabolism of compound A in humans has proved to be difficult. Experiments with human intestinal microsomes or intestinal slices did not indicate extensive glucuronidation, but the compound also had a low liver microsomal CL_{int}, contrary to the observation *in vivo*. However, evidence of intestinal metabolism of this compound came from the calculation of metabolite : parent drug ratios from the AUCs of plasma profiles. The AUCs from the time series of plasma drug and glucuronide concentrations after 100 mg intravenous administration (figure 10a) and 500 mg oral administration (figure 10b) were employed to obtain the metabolite : parent drug ratios (table IV). The fraction of the parent drug that is converted to the metabolite in the systemic circulation is obtained through division of the AUC calculated for the metabolite curve by the sum of the AUCs calculated for the parent drug and metabolite. Similarly, the fraction of the parent drug in the systemic circulation could also be estimated. The AUCs were computed by applying the trapezoidal rule to concentration-time values. The fractions of the parent drug and metabolite thus computed for the intravenous (figure 10a) and oral (figure 10b) curves and their corresponding metabolite : parent drug ratio are shown in table IV. A rough estimate of the metabolite : parent drug ratio that one would expect if there was no intestinal metabolism was also calculated for oral administration. If there was no intestinal metabolism, then the compound would be 100% absorbed (the result from PBPK simulations without inclusion of intestinal loss constants), as would be expec-

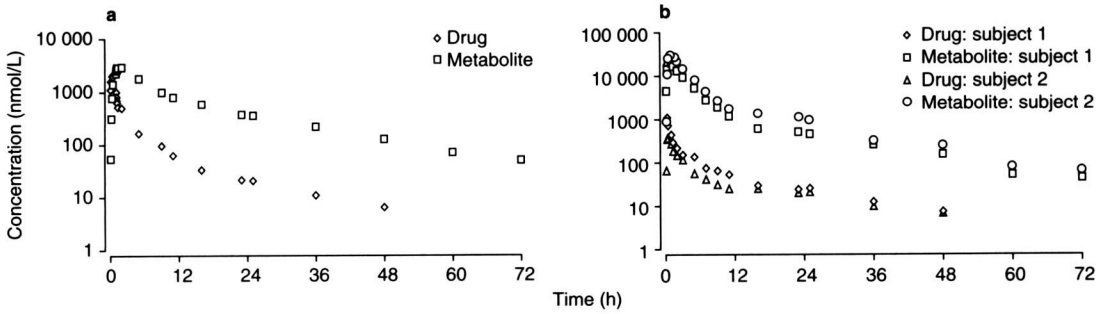

Fig. 10. Concentration-time profiles of the major metabolite (glucuronide) and the parent drug following (**a**) intravenous administration of 100 mg of compound A in one subject and (**b**) oral administration of 500 mg of compound A in two subjects.

Table IV. Metabolite : parent drug (M/P) ratios in humans for compound A

Mode of drug administration	Mean fraction of metabolite	Mean fraction of parent drug	M/P ratio
Intravenous (from AUC determination)	0.87	0.13	6.7
Oral (from AUC determination)	0.983	0.017	57
Oral (expected assuming there is no intestinal metabolism)			
after first pass	0.55	0.45	
during systemic circulation	0.39 (0.45 × 0.87)	0.06 (0.45 × 0.13)	
total	0.94 (0.39 + 0.55)	0.06	16

AUC = area under the plasma concentration-time curve.

ted from a compound with good permeability and solubility. Additionally, the compound has been shown to be chemically stable, and P-gp has been shown to be saturated at the high dose employed in the study. Using the calculated hepatic extraction ratio of 0.55, it is therefore reasonable to assume that the fraction of the parent drug that reaches the systemic circulation is 0.45. Once in the systemic circulation, 87% of the parent drug is likely to be converted to the metabolite, making the total metabolite fraction in the systemic circulation 0.94 (table IV). Only 13% of the parent drug that reaches the systemic circulation remains unchanged. Thus the fraction of the parent drug in plasma should be around 0.06 (0.13 × 0.45). The metabolite : parent drug ratio then becomes 16 (0.94 : 0.06). This is what one would expect for oral administration if there was no intestinal metabolism. However, the observed metabolite : parent drug ratio of 57 is significantly higher than the expected value of 16. The glucuronide concentrations observed after oral administration far exceeded the amounts that would be expected from hepatic extraction alone, thus providing proof of intestinal metabolism of compound A.

Discussion

The examples in this article used optimized distribution and clearance parameters from fitting intravenous profiles to understand the mechanisms underlying oral lineshapes. These examples serve to demonstrate that a lack of knowledge of tissue partition coefficients and CL_{int} need not limit application of PBPK simulations for deriving maximum information from pharmacokinetic profiles.

The role of the gut in limiting the bioavailability of some compounds has only recently been recognized as important.[47] Since the easily saturable P-gp is not likely to play a key role in affecting the bioavailability of a compound, intestinal metabolism may be an important factor for compounds with low bioavailability. It is impossible to estimate the absorption kinetics of a compound from its pharmacokinetic data without resorting to AUC comparisons of the parent and metabolite in the intravenous and oral routes. The deconvolution of absorption kinetics from the pharmacokinetic profiles is, however, easily achieved with PBPK simulations, meaning that it is possible to distinguish between intestinal extraction and hepatic extraction. Identifying the source of poor bioavailability is the crucial first step to focus on the right factors to improve bioavailability and therefore to avert a costly failure. It should be emphasized, however, that PBPK simulations cannot distinguish between gut wall metabolism, P-gp efflux or chemical degradation as the cause of intestinal loss. It is then important to resort to suitable experiments to eliminate mechanisms that are not probable for the compound of interest. For example, a compound with a high therapeutic dose is likely to saturate P-gp, which has a rather low Km value. This can be verified with knockout mice experiments. If the compound has also tested satisfactorily for chemical stability, then the cause of the intestinal loss is likely to be gut wall metabolism. Wu et al.[48] have described an experimental method in which concomitant administration of an enzyme inhibitor acting on the enzymes responsible for gut wall metabolism of the compound helped to differentiate oral drug loss due to gut wall metabolism.

Intestinal metabolism of both verapamil and compound A shows considerable variability with respect to species. The large interspecies variability that characterizes intestinal metabolism has been reported in the literature for several intestinally cleared compounds.[12,13,18] It is then possible that a compound that has acceptable bioavailability in preclinical species and has progressed to development could have poor bioavailability in humans. This was the case with compound A.

Understanding the role of the GI tract in determining the low and variable bioavailability of orally administered drugs is one important application of identification of intestinal loss with PBPK simulations. Another application could be prediction of concentrations reaching the liver after oral absorption, which is important for assessing the relevance of drug-drug interaction in the liver.[49] Also, recognition that a compound is actually metabolized in the gut and not only in the liver is crucial to ensuring that toxic effects of the metabolites on the GI tract are duly assessed.

Enterohepatic recirculation and drug-induced gastric emptying delay were discussed in this article only for the sake of completion of the lineshape analysis, and thus no supporting evidence for these pharmacokinetic processes has been provided.

Conclusion

Pharmacokinetic lineshapes contain information that can be valuable in understanding the underlying mechanisms. Routine application of PBPK simulations to pharmacokinetic profiles can bring to light information that can otherwise be lost. Verapamil is known to exhibit drug-induced impairment of gastric emptying, as well as gut wall metabolism. This article shows that doing simple lineshape simulations with PBPK can easily identify these pharmacokinetic processes. Similar principles applied to an in-house compound that was withdrawn from development demonstrated the usefulness of PBPK simulations to identify potential pharmacokinetic issues in drug development. In the absence of good experimental methods to identify intestinal loss, this article shows that PBPK simulations of human pharmacokinetic profiles provide a simple yet reliable alternative. The study highlights the need to do PBPK simulations on human oral pharmacokinetic profiles, as large interspecies variability in pharmacokinetic mechanisms can make interspecies extrapolation irrelevant. The examples in this article also demonstrate that lack of accurate inputs for clearance and distribution need not limit the application of PBPK in drug discovery and development projects.

Acknowledgements

The author sincerely thanks Dr Boel Löfberg of Discovery DMPK and Bioanalytical Chemistry, AstraZeneca, (Mölndal, Sweden) for providing the rat *in vitro* and *in vivo* preclinical pharmacokinetic data for compound A; Drs Susanne A. Johansson and Sophie Bååthe of the Clinical Pharmacology Department, AstraZeneca, for the human data for this compound; and Dr Hugues Dolgos and Associate Professor Anna-Lena Ungell of Discovery DMPK and Bioanalytical Chemistry, AstraZeneca R&D, for their helpful comments on the manuscript. No sources of funding were used to assist in the preparation of this study. The author has no conflicts of interest that are directly relevant to the content of this study.

References

1. Zhang Y, Benet LZ. The gut as barrier to drug absorption: combined role of cytochrome P450 and P-glycoprotein. Clin Pharmacokinet 2001; 40: 159-68
2. Christians U, Schmitz V, Haschke M. Functional interaction between P-glycoprotein and CYP3A in drug metabolism. Expert Opin Drug Metab Toxicol 2005; 1: 641-54
3. Ito K, Kusuhara H, Sugiyama Y. Effects of intestinal CYP3A4 and P-glycoprotein on oral drug absorption: theoretical approach. Pharm Res 1999; 16: 225-31
4. Lee YJ, Chung SJ, Shim CK. Limited role of P-glycoprotein in the intestinal absorption of cyclosporin A. Biol Pharm Bull 2005; 28: 760-3
5. Saitoh H, Saikachi Y, Kobayashi M, et al. Limited interaction between tacrolimus and P-glycoprotein in the rat small intestine. Eur J Pharm Sci 2006; 28: 34-42
6. Cao X, Yu LX, Barbaciru C, et al. Permeability dominates the *in vivo* intestinal absorption of P-gp substrate with high solubility and high permeability. Mol Pharm 2004; 2: 329-40
7. Kwon H, Lionberger RA, Yu LX. Impact of P-glycoprotein-mediated intestinal efflux kinetics on oral bioavailability of P-glycoprotein substrates. Mol Pharm 2004; 1: 455-65
8. Ogihara T, Kamiya M, Ozawa M, et al. What kinds of substrates show P-glycoprotein-dependent intestinal absorption? Comparison of verapamil and vinblastine. Drug Metab Pharmacokinet 2006; 21: 238-44
9. Krishna DR, Klotz U. Extrahepatic metabolism of drugs in humans. Clin Pharmacokinet 1994; 26: 144-60
10. de Waziers I, Cugnenc PH, Yang CS, et al. Cytochrome P450 isozymes, epoxide hydrolase and glutathione transferasesin rat and human hepatic and extrahepatic tissues. J Pharmacol Exp Ther 1990; 253: 387-94
11. Kaminsky LS. Small intestinal cytochromes P450. Toxicology 1992; 21: 407-22
12. Prueksaritanont T, Gorham LM, Hochman JH, et al. Comparative studies of drug-metabolising enzymes in dog, monkey, and human small intestines, and in Caco-2 cells. Drug Metab Dispos 1996; 24: 634-42
13. Kaji H, Kume T. Glucuronidation of 2-(4-chlorophenyl)-5-(2-furyl)-4-oxazoleacetic acid (TA-1801A) in humans: species differences in liver and intestinal microsomes. Drug Metab Pharmacokinet 2005; 20: 206-11
14. von Richter O, Burk O, Fromm MF, et al. Cytochrome P450 3A4 and P-glycoprotein expression in human small intestinal enterocytes and hepatocytes: a comparative analysis in paired tissue specimens. Clin Pharmacol Ther 2004; 75: 172-83
15. Zhang Q, Dunbar D, Ostrowska A, et al. Characterization of human small intestinal cytochrome P-450. Drug Metab Dispos 1999; 27: 804-9
16. Lin JH, Chiba M, Baillie TA. Is the role of small intestine in first pass metabolism overemphasized? Pharmacol Rev 1999; 51: 135-58
17. van Herwaarden AE, Wagenaar E, van der Kruijssen CM, et al. Knockout of cytochrome P450 3A yields new mouse models for understanding xenobiotic metabolism. J Clin Invest 2007; 117: 3583-92
18. van de Kerkhof EG, Ungell AL, Sjöberg AK, et al. Innovative methods to study human intestinal drug metabolism *in vitro*: precision-cut slices compared with Ussing chamber preparations. Drug Metab Dispos 2006; 34: 1893-902
19. Lindell M, Karlsson MO, Lennernas H, et al. Variable expression of CYP and Pgp genes in the human small intestine. Eur J Clin Invest 2003; 33: 493-9
20. Hilgendorf C, Ahlin G, Seithel A, et al. Expression of thirty-six drug transporter genes in human intestine, liver, kidney, and organotypic cell lines. Drug Metab Dispos 2007; 35: 1333-40
21. von Richter O, Greiner B, Fromm MF, et al. Determination of *in vivo* absorption, metabolism, and transport of drugs by the human intestinal wall and liver with a novel perfusion technique. Clin Pharmacol Ther 2001; 70: 217-27
22. Johnson BM, Chen W, Borchardt RT, et al. A kinetic evaluation of the absorption, efflux, and metabolism of verapamil in the autoperfused rat jejunum. J Pharmacol Exp Ther 2003; 305: 151-8
23. Glaeser H, Seigfried D, Hoffmann U, et al. Impact of concentration and rate of intraluminal drug delivery on absorption and gut wall metabolism of verapamil in humans. Clin Pharmacol Ther 2004; 76: 230-8
24. Theil FP, Guentert TW, Haddad S, et al. Utility of physiologically based pharmacokinetic models to drug development and rational drug discovery candidate selection. Toxicol Lett 2003; 138: 29-49
25. Christian L, Andreas R. Development and application of physiologically based pharmacokinetic modelling tools to support drug discovery. Chem Biodivers 2005; 2: 1462-86
26. Bernareggi A, Rowland M. Physiologic modeling of cyclosporin kinetics in rat and man. J Pharmacokinet Biopharm 1991; 19: 21-50
27. Peters SA. Evaluation of a generic physiologically based pharmacokinetic model for lineshape analysis. Clin Pharmacokinet 2008; 47: 261-75
28. Eichelbaum M, Mikus G, Vogelgesang B. Pharmacokinetics of (+)-, (-)- and (+/-)-verapamil after intravenous administration. Br J Clin Pharmacol 1984; 17: 453-8
29. Hanada K, Akimoto S, Mitsui K, et al. Enantioselective tissue distribution of the basic drugs disopyramide, flecainide and verapamil in rats: role of plasma protein and tissue phosphatidylserine binding. Pharm Res 1998; 15: 1250-6
30. Avdeef A, Artursson P, Neuhoff S, et al. Caco-2 permeability of weakly basic drugs predicted with the double-sink PAMPA pKa (flux) method. Eur J Pharm Sci 2005; 24: 333-49
31. Winiwarter S, Bonham NM, Ax F, et al. Correlation of human jejunal permeability (*in vivo*) of drugs with experimental and theoretically derived parameters: a multivariate data analysis approach. J Med Chem 1998; 41: 4939-49
32. Bhatti MM, Foster RT. Pharmacokinetics of the enantiomers of verapamil after the intravenous and oral administration of racemic verapamil in a rat model. Biopharm Drug Dispos 1997; 18: 387-96
33. Busse D, Templin S, Mikus G, et al. Cardiovascular effects of (R)- and (S)-verapamil and racemic verapamil in humans: a placebo-controlled study. Eur J Clin Pharmacol 2006; 62: 613-9
34. McAllister RG, Kirsten EB. The pharmacology of verapamil: IV. Kinetic and dynamic effects after single intravenous and oral doses. Clin Pharmacol Ther 1982; 31: 418-26

35. Björkman S, Stanski DR, Harashima H, et al. Tissue distribution of fentanyl and alfentanil in the rat cannot be described by a blood flow limited model. J Pharmacokinet Biopharm 1993; 21: 255-79
36. Peters SA, Hultin L. Early identification of drug-induced impairment of gastric emptying through physiologically based pharmacokinetic (PBPK) simulation of plasma concentration-time profiles in rat. J Pharmacokinet Pharmacodyn. Epub 2007 Oct 26
37. Brage R, Cortijo J, Esplungues J, et al. Effects of calcium channel blockers on gastric emptying and acid secretion of the rat *in vivo*. Br J Pharmacol 1986; 89: 627-33
38. Yavorsky RT, Hallgren SE, Blue PW. Effects of verapamil and diltiazem on gastric emptying in normal subjects. Dig Dis Sci 1991; 36: 1274-6
39. Krevsky B, Maurer AH, Niewiarowski T, et al. Effect of verapamil on human intestinal transit. Dig Dis Sci 1992; 37: 919-24
40. Tsimmerman IaS, Budnik IuB, Syman LN. The effect of calcium antagonists and beta-adrenoblockaders on disordered stomach functions in patients with duodenal peptic ulcer [in Russian]. Ter Arkh 1994; 66: 47-52
41. King CD, Rios GR, Green MD, et al. UDP-glucuronosyltransferases. Curr Drug Metab 2000; 1: 143-61
42. Fisher MB, Paine MF, Strelevitz TJ, et al. The role of hepatic and extrahepatic UDP-glucuronosyltransferases in human drug metabolism. Drug Metab Rev 2001; 33: 273-97
43. Strassburg CP, Kneip S, Topp J, et al. Polymorphic gene regulation and interindividual variation of UDP-glucuronosyltransferase activity in human small intestine. J Biol Chem 2000; 275: 36164-71
44. Sabolovic N, Heydel JM, Li X, et al. Carboxyl nonsteroidal anti-inflammatory drugs are efficiently glucuronidated by microsomes of the human gastrointestinal tract. Biochim Biophys Acta 2004; 1675: 120-9
45. Ghosal A, Hapangama N, Yuan Y, et al. Identification of human UDP-glucuronosyltransferase enzyme(s) responsible for the glucuronidation of ezetimibe (Zetia). Drug Metab Dispos 2004; 32: 314-20
46. Mistry M, Houston JB. Gluronidation *in vitro* and *in vivo*: comparison of intestinal and hepatic conjugation of morphine naloxone and buprenorphine. Drug Metab Dispos 1987; 15: 710-7
47. Kaminsky LS, Zhang Q-Y. The small intestine as a xenobiotic-metabolizing organ. Drug Metab Dispos 2003; 31: 1520-5
48. Wu C-Y, Benet LZ, Hebert MF, et al. Differentiation of absorption and first-pass gut and hepatic metabolism in humans: studies with cyclosporine. Clin Pharmacol Ther 1995; 58: 492-7
49. Rodrigues AD, Winchell GA, Dobrinska MA. Use of *in vitro* drug metabolism data to evaluate drug-drug interactions in man: the need for quantitative databases. J Clin Pharmacol 2001 41: 368-373

Correspondence: Dr *Sheila Annie Peters*, Discovery DMPK and Bioanalytical Chemistry, AstraZeneca R&D, Pepparedsleden 1, 43151 Mölndal, Sweden. E-mail: sheila.peters@astrazeneca.com